DTU Library

Test of Heliac 3rd Gen. Solar Collector

Solar Collector Thermal Performance and Pressure Drop Test based on ISO 9806:2017

Jensen, Adam R.

Publication date:
2020

Document Version
Publisher's PDF, also known as Version of record

DTU Civil Engineering
Department of Civil Engineering

BYG R-443
September 2020

Test of Heliac 3rd Gen. Solar Collector

Solar Collector Thermal Performance and Pressure Drop Test according to ISO 9806:2017

Adam R. Jensen

Test of Heliac 3rd Gen. Solar Collector

Solar Collector Thermal Performance and Pressure Drop Test based on ISO 9806:2017

Report
September 2020

By
Adam R. Jensen

Cover photo: Photo of the Heliac solar collector field at Lendemarke.

Published by: DTU, Department of Civil Engineering, Brovej, Building 118, 2800 Kgs. Lyngby Denmark
www.byg.dtu.dk

ISBN: 87-7877-544-2

Byg report: R-443

Contents

This page has been intentionally left blank.

Nomenclature

Symbol	Description	Unit
A	Aperture area	m^2
a_1	Heat loss coefficient	$W/(m^2\ K)$
a_2	Temperature dependence of the heat loss coefficient	$W/(m^2\ K^2)$
a_3	Wind speed dependence of the heat loss coefficient	$J/(m^3\ K)$
a_5	Effective thermal capacity	$J/(m^2\ K)$
a_6	Wind speed dependence of the zero-loss efficiency	s/m
a_7	Wind speed dependence of the IR radiation exchange	s/m
a_8	Radiation losses	$W/(m^2\ K^4)$
E_L	Longwave irradiance (λ > 3 μm)	W/m^2
G_b	Direct solar irradiance (beam irradiance)	W/m^2
G_d	Diffuse solar irradiance	W/m^2
G_{hem}	Hemispherical solar radiation	W/m^2
$K_b(\theta_L, \theta_T)$	Incidence angle modifier for direct solar irradiance	-
K_d	Incidence angle modifier for diffuse solar radiation	-
ΔP	Pressure drop	bar
$\dot{Q}$	Useful power extracted from collector	W
T_{amb}	Ambient air temperature	°C
T_{in}	Collector inlet temperature	°C
T_{out}	Collector outlet temperature	°C
T_{mean}	Mean temperature of heat transfer fluid	°C
$\dot{V}$	Volume flow rate	m^3/h
$\eta_{0,b}$	Peak collector efficiency ($T_{mean} - T_{amb} = 0$) based on beam irradiance G_b	-
u	Surrounding airspeed	m/s
σ	Stefan-Boltzmann constant	$W/(m^2\ K^4)$

1. Method

This test report presents the methodology and results of the thermal performance and pressure drop test of the 3rd generation Heliac solar collector. The tested collector features the third version of Heliac's Fresnel lenses with the SafeLens design and receivers coated with Pyromark paint.

The solar collector was installed and tested at the Department of Civil Engineering's experimental facility at the Technical University of Denmark in Lyngby, Denmark. The Heliac solar tracker, including glass frames and piping, was already installed onsite during a previous project. Thus, for the test of the 3rd generation solar collector, only the lenses and receivers were exchanged by Heliac.

The thermal performance of the solar collector was determined using the quasi-dynamic test (QDT) method based on outdoor measurements. Additionally, the pressure drop over the collector was measured and characterized. Both tests were made according to the international standard ISO 9806:2017 (International Standard, 2017).

The thermal performance tests were performed between June 9th and June 24th, 2020. No preconditioning of the solar collector was done before the thermal performance test. The pressure drop measurements were made on July 13th, 2020.

Test description

Method:	Outdoor thermal performance characterization using the quasi-dynamic test method and pressure drop test according to ISO 9806:2017
Period:	June 2020
Responsible:	Adam R. Jensen

Collector description

Manufacturer:	Heliac ApS info@heliac.dk Savsvinget 4D 2970 Hørsholm, Denmark
Collector type:	Fresnel lens concentrating solar collector with two-axis tracking. Pyromark coated receivers and Heliac's 3rd generation Fresnel lens.
Aperture area:	16.55 m^2
Installation date:	Lenses (May 13th 2020), receivers (June 2nd 2020)

2. Method

Thermal performance testing is conducted to determine a set of coefficients, with which it is possible to describe the collector power output for the entire range of operating conditions. For concentrating solar collectors, the coefficients can be determined using the *quasi-dynamic test (QDT) method for liquid heating collectors*. This method has been adopted as an international standard and is documented in ISO 9806:2017 (International Standard, 2017).

The QDT method describes the collector power output using the following equation:

$$\begin{aligned}\dot{Q} = A\,\big[\eta_{0,b}\,K_b(\theta_L,\theta_T)\;G_b + \eta_{0,b}\,K_d\,G_d - a_1\,(T_{mean} - T_{amb})\\ - a_2\,(T_{mean} - T_{amb})^2 - a_3\,u\,(T_{mean} - T_{amb}) + a_4\,(E_L - \sigma\,T_a^4)\\ - a_6\,u\,G_{hem} - a_7\,u\,(E_L - \sigma T_a^4) - a_8\,(T_{mean} - T_{amb})^4\big]\end{aligned} \quad \text{Eq. 1}$$

The equation relies on a number of collector coefficients, which are specific to each collector, to describe the heat gains and losses. The description and unit of each of the collector parameters in Equation 1 are listed in the nomenclature section. The coefficients are determined by fitting Equation 1 to measurement test data using statistical least square curve fitting. It is important to collect high-quality measurement data of the collector power output and ancillary variables, which should include sufficient variation of the operating conditions.

Measurement data was obtained by testing Heliac's 3rd generation solar collector at DTU Civil Engineering's experimental test facility from June 9th to June 24th 2020. During this period the inlet temperature of the collector was varied between 18°C and 80°C. The collector was tested with water as the heat transfer fluid, which is the industry standard, as the uncertainty of the results is increased when testing with glycol or other additives. ISO 9806 recommends testing at a flow rate of 0.02 kg/s per square meter of gross collector area, which corresponded to 21 L/min in this test. However, due to limitations of the test setup, the collector was operated with a constant volume flow rate of 17 L/min (1.02 m^3/hr) for the entire test period.

Furthermore, it is important to check that the measurement data has sufficient variation between the measured parameters for the method to accurately determine the coefficients. This condition was checked using scatter plots that compared the measured parameters, shown in Figure 1.

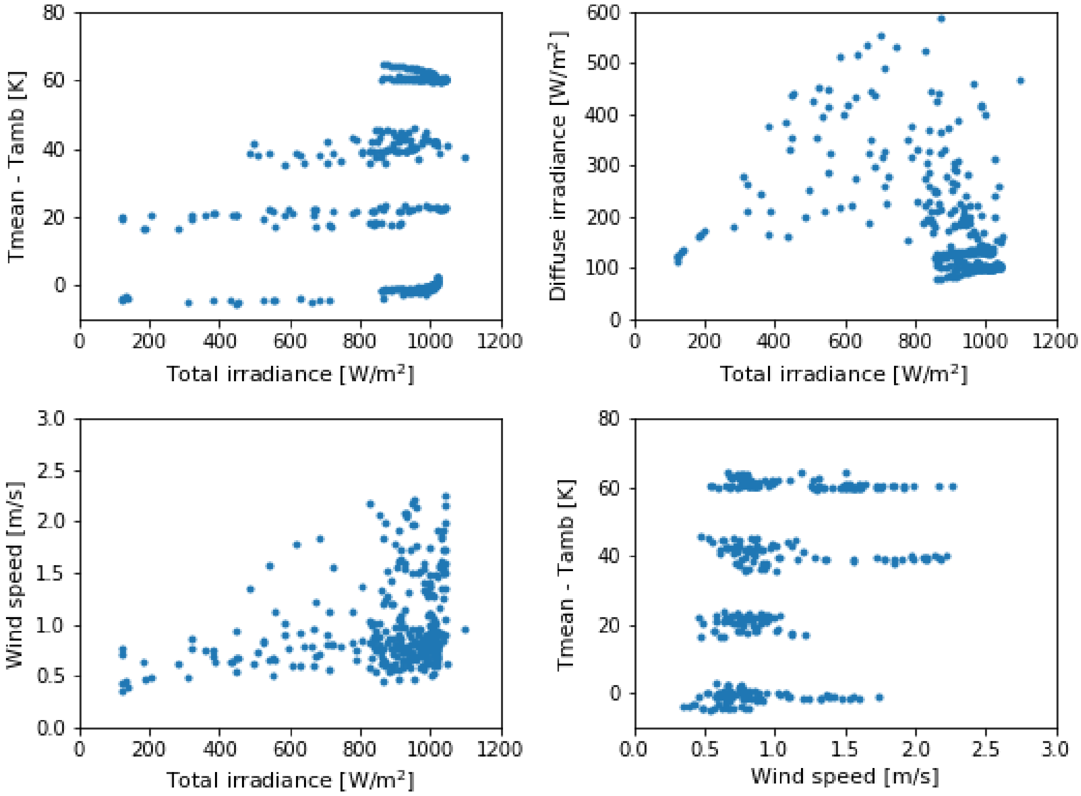

Figure 1: Comparison of the parameter variation of the measurement data.

In addition to thermal performance testing, the pressure drop over the collector was also quantified. This information is important when designing solar collector systems, as the pressure drop determines how many collectors can be put in series and the necessary pump power.

For the pressure drop tests, the collector was positioned pointing south with a tilt of 45 degrees. The fluid temperature was maintained at 60°C during the pressure drop tests. At this temperature, water has a dynamic viscosity of 0.466 mPa·s.

The pressure drop was measured using two pressure transducers installed immediately before the inlet and after the outlet of the collector. The pressure drop was then measured for seven different flow rates, ranging from 6 to 20 L/min (0.36 to 1.2 m^3/hr). For each flow rate, the average pressure drop was calculated for a stable period of at least 10 minutes.

The pressure drop coefficients (a and *b*) were determined by fitting the pressure drop measurements to Equation 2.

$$\Delta P = a\,\dot{V} + b\,\dot{V}^2 \qquad \text{Eq. 2}$$

The measurement equipment used for the thermal performance and pressure drop tests is listed in Table 1, along with the instruments' respective uncertainties. All of the instruments used satisfy the requirements of ISO 9806:2017.

Table 1: Measurement equipment and uncertainties.

Measurement	Equipment manufacture and model	Uncertainty
Direct irradiance	Kipp & Zonen CHP1 pyrheliometer	Class A
Global irradiance	Kipp & Zonen SMP10 pyranometer	Class A
Temperature	Endress+Hauser TST310 PT100	0.2 K (absolute) 0.05 K (differential)
Flow rate	Krohne Optiflux 1050	0.5 %
Pressure	Krohne Optibar P 1010	0.25%
Wind speed/direction	Gill WindSonic ultrasonic anemometer	2% / 2°

3. Results

The main results from the thermal collector test are the collector coefficients, listed in Table 2. With these coefficients and the use of Equation 1, it is possible to calculate the expected thermal output of the Heliac collector for any combination of operating conditions within the tested range. This is especially useful in predicting the expected power output of solar collector fields or for comparing different solar collectors.

Table 2: Collector performance coefficients derived using the QDT method.

Parameter	Value	Std. error	Unit
η_0	60.2%	0.1%	-
K_b	1	0	-
K_d	0.02	0.002	-
a_1	0.23	0.03	$\mathrm{W/(m^2\ K)}$
a_2	*		$\mathrm{W/(m^2\ K^2)}$
a_3	0.178	0.02	$\mathrm{J/(m^3\ K)}$
a_4	*		-
a_5	3357	141	$\mathrm{J/(m^2\ K)}$
a_6	*		$\mathrm{s/m}$
a_7	*		$\mathrm{s/m}$
a_8	*		$\mathrm{W/(m^2\ K^4)}$

Coefficients marked with an asterisk (*****) were not included, as they were found to be insignificant or irrelevant to the tested collector type.

As shown in Table 2, values were determined for η_0,K_b, K_d a_1, a_3, and a_5. The η_0 coefficient is also known as the optical efficiency, as this coefficient describes the fraction of the beam radiation that can be converted to heat by the receivers. It is an ideal efficiency, as it is only obtainable under conditions where there are no other losses, i.e., $T_{mean} = T_{amb}$. Due to the two-axis tracking of the collector, the incidence angle is always zero, and the beam incidence angle modifier, K_b, was set to 1.

Coefficients a_4 and a_7 are related to long-wave radiation exchange, which does not significantly affect concentrating collectors; thus, these coefficients were not determined. Furthermore, during the QDT procedure, the values for coefficients a_2, a_6, and a_8 were set to zero because they were either statistically insignificant or had a negative sign.

It is important to note that the coefficients in Table 2 are related to the aperture area, which was 16.55 m^2.

As previously mentioned, once the collector parameters have been determined, it is possible to calculate the expected thermal power output. In Table 3, this has been done for three different irradiance conditions: blue sky (1000 W/m^2), hazy sky (700 W/m^2), and grey sky (400 W/m^2). These three cases are known as Standard Reporting Conditions (SRC). The thermal power outputs for the Heliac collector under these conditions and with varying mean collector fluid temperatures are listed in Table 3.

Table 3: Collector power output under Standard Reporting Conditions (SRC). SRC assumes an ambient temperature of 20°C and a wind speed of 1.3 m/s. Nominal flow rate ($\dot{V}$=17 L/min).

T_{mean} [°C]	**Blue sky** 1000 W/m^2 G_b = 850 W/m^2 G_d = 150 W/m^2	**Hazy sky** 700 W/m^2 G_b = 440 W/m^2 G_d = 260 W/m^2	**Grey sky** 400 W/m^2 G_b = 0 W/m^2 G_d = 400 W/m^2
20	8499 W	4436 W	80 W
40	8346 W	4283 W	0 W
60	8193 W	4130 W	0 W
80	8040 W	3977 W	0 W
110	7811 W	3748 W	0 W

The power output for STC is also graphically illustrated in Figure 2. The slope of the power output curves is rather small, indicating a low heat loss from the collector. It is also evident from Table 3 and Figure 2 that the Heliac collector essentially does not produce any useful heat under grey sky conditions. This is because the collector is a concentrating collector, which predominantly uses beam radiation, only present in clear and hazy sky conditions.

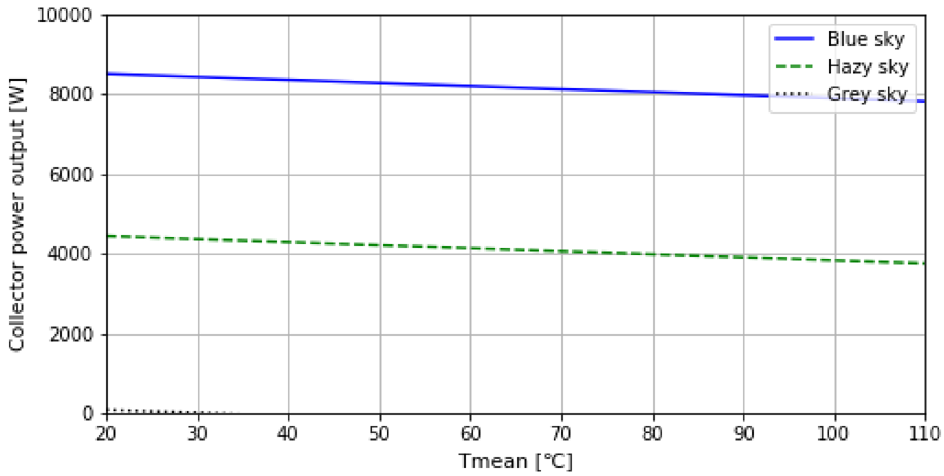

Figure 2: Collector power output under standard reference conditions.

As an example, the collector coefficients presented in Table 2 have been applied using Equation 1 to calculate the thermal power output for a cloudy and clear sky day. The results for the cloudy day are shown in Figure 3 and the results from the clear sky day are shown in Figure 4. Both figures also include measurement data of the hemispherical, beam, and diffuse irradiances and inlet, outlet, and ambient temperatures.

The irradiance for the cloudy day, shown in the middle subplot in Figure 3, fluctuates greatly during the day due to drifting clouds and intermittent periods with clear skies. As a result, the power output, shown in the top subplot, also fluctuates. By comparing the two curves, it is evident that the derived QDT coefficients are able to accurately model the power output.

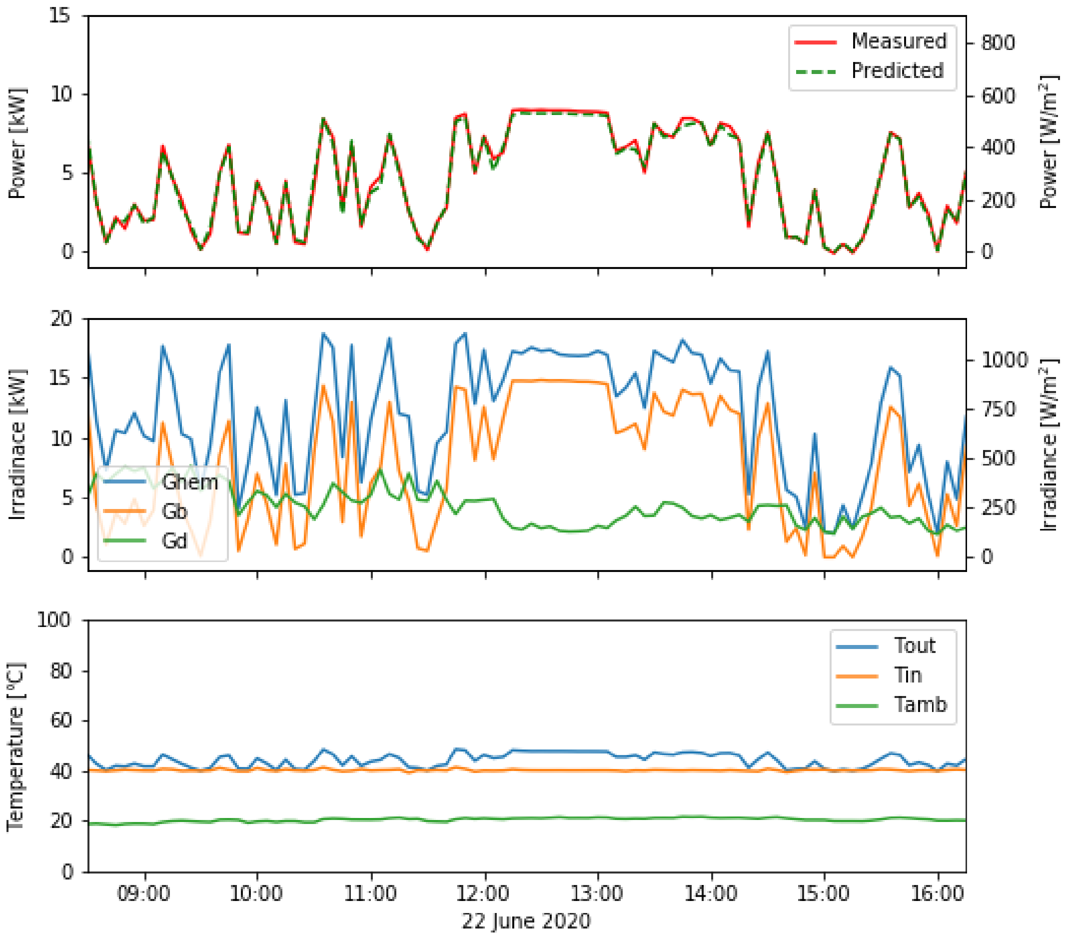

Figure 3: Measurement data and predicted power output for a day with drifting clouds.

Similarly, in Figure 4, the measurements and predicted power for a clear sky day are presented. During this day the irradiance only changed gradually and was dominated by beam radiation; thus, the collector outlet temperature was practically constant. Furthermore, due to the two-axis tracking of the collector, the power output was relatively constant during the day.

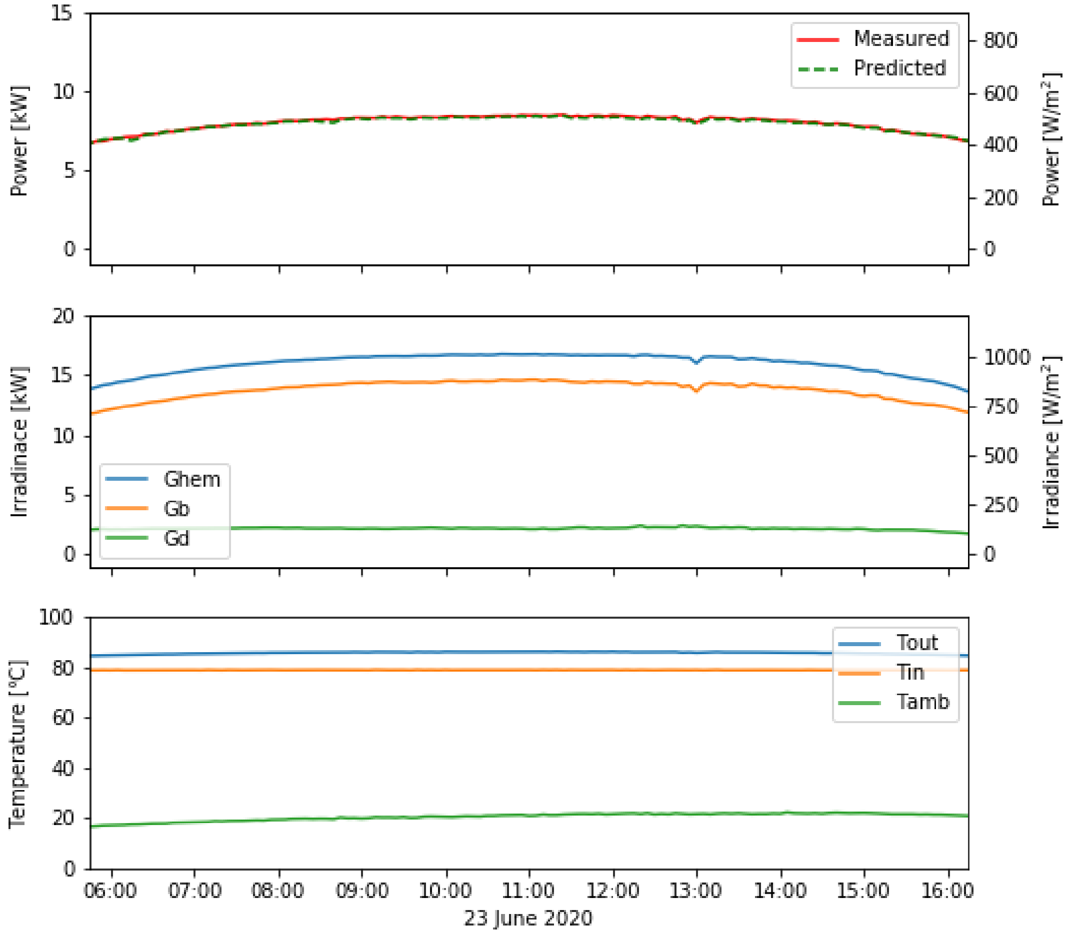

Figure 4: Measurement data and predicted power output for a clear sky day.

As mentioned in Section 2, the pressure drop was measured under steady-state conditions for seven different flow rates. The flow rates and measured pressure drop are listed in Table 4.

Table 4: Collector pressure drop vs. flow rate.

Flow rate (m^3/h)	0.36	0.48	0.60	0.72	0.90	1.02	1.19
Pressure drop (bar)	0.09	0.14	0.20	0.28	0.55	0.55	0.75

To be able to predict the pressure drop for any given flow rate through the collector, the two pressure drop coefficients, *a* and *b*, were fitted to Equation 2 using the data presented in Table 4. The pressure drop coefficients were found to be $a = 0.0431\ \mathrm{bar/(m^3/h)}$ and $b = 0.4917\ \mathrm{bar/(m^6/h^2)}$. The resultant regression curve and the measured pressure drops are shown in Figure 5.

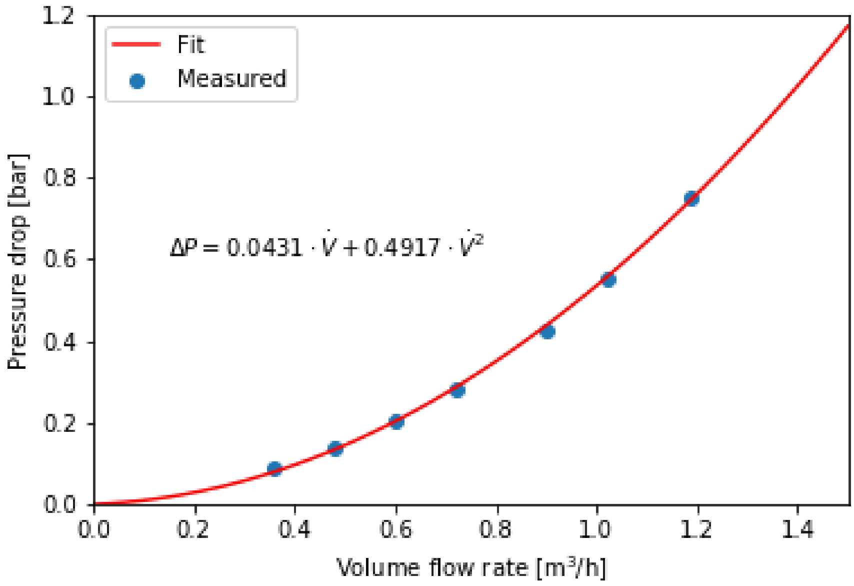

Figure 5: Pressure drop regression curve and measured values.

References

International Standard, 2017. ISO 9806:2017 Solar energy-Solar thermal collectors-Test methods.

DTU Civil Engineering
Department of Civil Engineering

BYG R-443
September 2020

ISBN: 87-7877-544-2

Department of Civil Engineering, DTU
Brovej, Building 118
2800 Kgs. Lyngby

www.byg.dtu.dk/english
Tel: 4525 1700